A simple nanostructured polymer/ZnO hybrid solar cell - preparation and operation in air

Krebs, Frederik C; Thomann, Yi; Thomann, Ralf; Andreasen, Jens Wenzel

Published in:
Nanotechnology

Link to article, DOI:
10.1088/0957-4484/19/42/424013

Publication date:
2008

A simple nanostructured polymer/ZnO hybrid solar cell – preparation and operation in air

Frederik C. Krebs*[,a], Yi Thomann[b], Ralf Thomann[b] and Jens W. Andreasen[a]

[a]*Risø National Laboratory for Sustainable Energy, Technical University of Denmark, Frederiksborgvej 399, DK-4000 Roskilde, Denmark.*

[b] *Freiburger Materialforschungszentrum, University of Freiburg, Stefan Meier Straße 21, 79104 Freiburg, Germany.*

e-mail: frederik.krebs@risoe.dk

Abstract

A detailed description of the preparation of a polymer solar cell and its characterization is given. The solar cell can be prepared entirely in the ambient atmosphere by solution processing without the use of vacuum coating steps and can be operated in the ambient atmosphere with good operational stability under illumination (1000 W m^{-2}, AM1.5G, 30 ^{o}C, 35 ± 5 % relative humidity) for 100 hours with a 20% loss in efficiency with respect to the initial performance. The dark storability (darkness, 25 ^{o}C, 35 ± 5 % relative humidity) has been shown to exceed six months without notable loss in efficiency. The devices do not require any form of encapsulation to gain stability while a barrier for mechanical protection may be useful. The devices are based on soluble zinc oxide nanoparticles mixed with the thermocleavable conjugated polymer poly-(3-(2-methylhexan-2-yl)-oxy-carbonyldithiophene) (P3MHOCT) that through a thermal treatment is converted to the insoluble form poly(3-carboxydithiophene) (P3CT) that generally gives stable polymer solar cells. The devices employed a solution based silver back electrode. One advantage

is that preparation of the devices is very simple and can be carried out by hand under ambient conditions requiring only a hot plate that can reach a temperature of 210 ^{o}C and preferably also a spincoater. This type of device is thus excellently suited for teaching and demonstration purposes provided that the materials are at hand.

1. Introduction

The examples of solar cells wherein organic molecules are responsible for the light harvesting and charge carrier generation fall into the four broad categories of dye sensitized solar cells (DSSC, Grätzel cells) [1,2], small molecule [3,4], polymer solar cells [5,6] and hybrid solar cells [7,8]. The power conversion efficiency that can be achieved with each of these technologies is highest for the DSSCs (~11%) [9] and similar for the small molecule [10] organic and polymer solar cells [11,12] (~5% for single junctions). The DSSCs are by far the most popular type of organic solar cells in terms of the number of research papers, the documented attempts of commercialization and the general awareness of the technology. One could argue that the reason for this is that the achievable power conversion efficiency is approximately twice as high as for the other three categories but another and perhaps more disputable reason could be that they are quite simple to prepare using simple equipment and readily available materials. For these reasons they may have inspired many more people [13-15]. The DSSCs have been prepared by school classes employing window glass, white paint, a kitchen oven and some sort of colored dye from berries or wine. This is not to say that the DSSCs prepared in this manner achieve a high power conversion efficiency or that they are particularly stable in operation, but the DSSC's excel when it comes to power conversion efficiency, simplicity and ease of demonstration. It is difficult to envisage a more powerful example where the lay man with simple prerequisites can prepare a

working piece of nanotechnology. By comparison small molecule, polymer and hybrid solar cells all require access to complex materials, substrates, high vacuum equipment and special inert atmosphere processing conditions. One could hold these facts as the main reasons that the latter three technologies are not as widespread (not even in academic circles).

In this work we demonstrate a nanostructured polymer hybrid solar cell with excellent operational stability that can be prepared in the ambient atmosphere by simple means. There is a requirement for materials with a certain level of complexity but there are no requirements for vacuum or inert processing conditions. It is our hope that this example can be used by school or university classes for the preparation and demonstration of the polymer and hybrid solar cell technology.

2. Experimental

All handling and preparation was in ambient air, no inert gasses or special precautions were made to protect the materials, substrates and cells from oxygen and water in the atmosphere during handling and processing. The manipulations were carried out at an ambient temperature of 20 ± 2 ^{o}C and a relative humidity of 35 ± 5 %.

2.1 Substrates

Conducting indium tin-oxide substrates were employed. Rigid glass substrates with a 100 nm layer of ITO and a sheet resistivity of 8-12 Ω square^{-1} were purchased from Lumtec and were cleaned by consecutive ultrasonication in acetone, water and isopropanol for 5 min followed by drying immediately prior to use. The flexible substrates were purchased from Delta Technologies and comprised 200 micron polyethyleneterephthalate (PET) foil with an overlayer of ITO and a

sheet resistivity of 25-35 Ω square^{-1}.The cleaning procedures were useful for the achievement of reproducible results but can be avoided.

2.2 Zinc oxide nanoparticles

The zinc oxide nanoparticles were prepared by a procedure similar to the one reported in the literature [16-20]. In a typical run starting from $Zn(OAc)_2{\cdot}2H_2O$ (29.7g) in methanol (1250 mL) heated to 60 ^oC, KOH (15.1g) dissolved in methanol (650 mL) heated to 60 ^oC was added over 30 seconds. The mixture becomes cloudy towards the end of the addition. The mixture was heated to gentle reflux and after 2-5 minutes the mixture became clear and was stirred at this temperature for 3 hours during which time precipitation starts. The magnetic stirring bar was removed and the mixture left to stand at room temperature for 4 hours. The mixture was carefully decanted leaving only the precipitate. The precipitate was then resuspended in methanol (1 L) and allowed to settle for 16 hours. The methanol was removed by decantation making sure that the precipitate was drained as well as possible without letting it dry. Chlorobenzene (40 mL) was added immediately and the precipitated nanoparticles dissolved gradually over 15 minutes giving a total volume of 60 mL. The concentration was typically in the range 150-225 mg mL^{-1}. After determination of the zinc oxide concentration MEA was added. The best range of MEA concentrations was found to be 4-6% w/w with respect to zinc oxide. Concentrations as high as 20% w/w were employed and gave the highest stability for the zinc oxide nanoparticle solutions but as discussed in the following this had severe disadvantages in terms of making device films.

2.3 The materials for the active layer

Regiorandom poly-(3-(2-methylhex-2-yl)-oxy-carbonyldithiophene) (P3MHOCT) was prepared as described in the literature [21]. The polymer had the following properties: M_n = 11600 g mol^{-1},

M_w = 28300 g mol^{-1}, M_p = 27500 g mol^{-1}, PD = 2.6. P3MHOCT solutions in chlorobenzene were prepared by gentle shaking at room temperature for 6 hours (elevated temperatures were avoided). The final solution had a concentration of 25 mg mL^{-1} with respect to P3MHOCT and 50 mg mL^{-1} with respect to zinc oxide nanoparticles. The solution was microfiltered through a Teflon microfilter with a pore size of 0.45 micron. The solutions were stable for many weeks.

2.4 The PEDOT:PSS

Several types of PEDOT:PSS were employed with roughly equal success. The aqueous dispersion used for spincoating was purchased from Aldrich as a 1.3 wt % dispersion and used as received. The screen printable PEDOT:PSS was purchased from Agfa (Orgacon-5010). Screen printing was performed either manually or on a semiautomatic screen printing machine (AT701 from ALRAUN TECHNIK, Germany) with squeegee speeds of 550 mm s^{-1} and a 180 mesh screen. The typical sheet resistivities that could be obtained were 10 kΩ square^{-1} for the PEDOT:PSS spin coated from an aqueous dispersion and 500 Ω square^{-1} for a single layer of screen printed PEDOT:PSS. Three consecutively prepared prints gave a sheet resistivity of 110-130 Ω square^{-1}.

2.5 The back electrode

The silver back electrode was based on Dupont 5007 and is a silver migration resistant polymer thick film conductor that was cured at 130-140 ^{o}C for 3 minutes. The silver electrode was prepared by screen printing (120 mesh), by simple brushing with a paint brush or by casting through a mask. The typical sheet resistivities that could be obtained were < 1 Ω square^{-1}.

2.6 Preparation of devices on flexible and rigid conducting substrates

A 50 mg mL^{-1} zinc oxide solution stabilized with 4% w/w MEA was spincoated onto the substrates at 1000 rpm. The substrate was subsequently heated to polymerize the zinc oxide film and make it insoluble. This was easily tested by streaking a cotton bud wetted in chlorobenzene across the film. The film should not be affected by this treatment. In the case of the glass-ITO substrate heating to 310 ^{o}C on a hot plate for 5 minutes gave an isoluble film. In the case of the PET-ITO heating to 130 ^{o}C for 5 hours was required and only partial insolubility was achieved such that the films withstood chlorobenzene solvent for brief periods of time (ie. during spincoating) but was removed upon mechanical abrasion with a cotton bud wetted with chlorobenzene. For the patient experimenter it is advantageous to subject the samples to a thermal treatment (130 ^{o}C for 3-5 hours) followed by storage at ambient conditions overnight (10-16 hours). The MEA stabilized P3MHOCT-zinc oxide solution was then spincoated on top of the zinc oxide layer and should give a clear film. Visible opacity of the film is due to an excess of MEA (se discussion section). The films were subsequently placed on a hot plate at a temperature of 210 ^{o}C whereby P3MHOCT is thermocleaved to P3CT. The transformation is rapid and clearly visible as a color change from dark red to a lighter red color. The transformation is complete in less then 5 minutes and the completion of the conversion can be checked with a cotton bud wetted with chlorobenzene which should leave the film insoluble and unscathed. In the case of PET substrates the films were kept in an oven at 140 ^{o}C where the conversion does take place albeit very slowly. The PET substrates were kept in the oven at 140 ^{o}C until the films were insoluble which typically required 16 hours. The devices were completed by spin coating an 1.3 wt% aqueous dispersion of PEDOT:PSS (at 2800 rpm) followed by drying at 120 ^{o}C for 10 minutes or by screen printing of Orgacon-5010 through a 140 mesh screen followed by drying at

120 ^{o}C for 15 minutes. The devices were completed by screen printing, painting or casting a Dupont 5007 layer defining the back electrode followed by heating to 130-140 ^{o}C for 5 minutes. The active area of the devices was 1 cm^2 squares.

2.7 X-ray scattering techniques and analysis

Samples representing the different components and processing steps were subjected to several complementary X-ray scattering techniques. Small Angle X-ray Scattering (SAXS) data were acquired for zinc oxide and P3MHOCT in solution, both separate and mixed (25 mg/ml ZnO and 12.5 mg/ml P3MHOCT in chlorobenzene). Small and Wide Angle X-ray data were acquired in grazing incidence (GISAXS/GIWAXS) as well as reflectivity profiles for thin films of zinc oxide, polymer and blend, as spun from the same solutions on silicon wafers and after annealing at 200°C. SAXS/GISAXS data were acquired using a fully evacuated small angle scattering camera with a gas proportional area detector 715 mm from the sample. The X-ray source is a rotating Cu-anode with fine focus filament, operated at 46 kV/64 mA, focused and monochromatized (Cu K_α, λ = 1.5418 Å) by a 2D graded and curved multilayer, and collimated by 3 pinholes. Total integration time was 2 hs for solution samples and 0.5 hs for thin film samples. The X-ray incidence angle for the GISAXS measurements was 0.5°, chosen as a compromise between sufficient intensity in the small angle scattering regime while minimizing intensity in the specularly reflected beam to avoid strong effects of multiple scattering [22]. Solution SAXS data were reduced from 2D scattering data to 1D cross sections by azimuthal averaging, and fitted by models describing polydisperse (Schulz distribution [23,24]) populations of spherical particles (for ZnO) or a combined Guinier/Porod function (for the polymer solution)

[25]. The GISAXS data were integrated in azimuthal sections of 5° around the Q_{xy} direction (in the substrate plane) to yield 1D scattering cross sections for quantification. The integrated data were fitted by models describing polydisperse populations of spherical particles with a hard-sphere potential [26] describing the particle interaction, as implemented in the program MIXTURE [27]. Integrating the intensity on the SAXS area detector as a function of incidence angle performed as a fast (18 minutes) reflectivity measurement. Because the specularly reflected intensity is much stronger than the diffuse scattering, this procedure yields acceptable reflectivity curves, adequate for thickness determination. Only a simple data analysis was carried out, determining the film thickness from the periodicity of the observed Kiessig fringes [28].

The GIWAXS measurements operate on the same principles as GISAXS, i.e. by orienting the substrate surface at or just below the critical angle with respect to the incoming beam, scattering from the deposited film is maximized with respect to scattering from the substrate. In the wide scattering angle range (>5°), the X-ray scattering is sensitive to crystalline structure. The GIWAXS data were acquired using a camera comprising an evacuated sample chamber with an X-ray photo-sensitive image plate with a rotating Cu-anode operating at 50 kV/200 mA as X-ray source, focused and monochromatized (Cu K_α, λ = 1.5418 Å) by a 1D multilayer [29]. Phase identification was accomplished by comparing azimuthal averages of the 2D data (equivalent of 2θ-scans) with tabulated data (powder diffraction file, PDF-2, 2003)

2.8 Microscopy techniques

Transmission electron microscopy (TEM) measurements were carried out with a Zeiss LEO 912 Omega transmission electron microscope applying an acceleration voltage of 120 keV. The specimens for particle analyses were made by evaporating a drop of particle suspension onto a carbon coated copper grid. Grids were plotted dry on a filter paper and investigated in the zero

loss filtered mode without further treatment. Film samples were removed from the glass substrate in water. Small pieces of the films were placed on 400 mesh copper grids and measured without further treatment. Atomic force microscopy (AFM) measurements of the films were employed to determine the film thickness. AFM experiments were performed with a Nanoscope III scanning probe microscope. The height images were obtained while operating the instrument in the tapping mode under ambient conditions. Images were taken at the fundamental resonance frequency of the Si cantilevers which was typically around 180 kHz. Typical scan speeds during recording were 0.3-1 line/s using scan heads with a maximum range of 16×16 µm.

2.9 Device testing and characterization

The devices were illuminated in the ambient atmosphere using a solar simulator from Steuernagel lichttechnik, KHS 575). The luminous intensity and emission spectrum of the solar simulator approaches AM1.5G and was set to 1000 W m^{-2} using a precision spectral pyranometer from Eppley Laboratories (www.eppleylab.com). The incident light intensity was monitored continuously every 60 seconds during the measurements using a CM4 high temperature pyranometer from Kipp & Zonen (www.kippzonen.com). Both instruments are bolometric. The variation in incident light intensity during the duration of the testing (140 hours) was less than 5% and no corrections were made. No corrections for mismatch were made. IV-curves were recorded with a Keithley 2400 Sourcemeter from -1V to + 1V in steps of 10 mV with a speed of 0.1 second $step^{-1}$ using custom made software. When testing the lifetime under accelerated conditions (1000 W m^{-2}, 72 ± 2 ^{o}C, ambient atmosphere, 35 ± 5 % humidity) the devices were kept under short circuit conditions and IV-curves were recorded from -1 V to +1 V every minute. The unencapsulated device was placed under the sun simulator during measurements.

3. Results and discussion

3.1 Background

It is of some interest to be able to prepare polymer solar cells in the ambient atmosphere without the need for vacuum coating steps. Ideally the solar cells should also exhibit some stability towards storage and operation in the ambient atmosphere without any form of encapsulation or extra precaution in terms of usable ranges of temperature or humidity. An example of such a polymer solar cell was described recently based on a bulk heterojunction between the polymer material P3CT and nanoparticles of zinc oxide [20]. While this device complies with the above desires it was best prepared in a glovebox environment. The reason for this was that the zinc oxide nanoparticle solutions were not stable in the ambient atmosphere with the solvent types required for preparation and processing of thin films. The preparation of smooth films was not possible unless inert atmospheres were used. The preparation of a stable form of the nanoparticles was thus the only requirement before air preparation could be envisaged.

3.2 Zinc oxide nanoparticles and preparation of films

The preparation of soluble forms of zinc oxide nanoparticles and sols has been described in a series of patents by Womelsdorf et al. [16-18] and later employed in hybrid cells with PPVs by Beek et al. [19] and this spawned research by numerous groups. The zinc oxide nanoparticles are in a soluble form when freshly prepared from methanol through methoxy groups being exposed at the surface (figure 1). In organic solvents they are readily soluble and the particles will not grow any further provided that water is excluded. If however methanol is lost from the surface or if water is admitted they will react and stick together. The methoxylated zinc oxide nanoparticles are not very stable in the presence of water and solid zinc oxide quickly precipitates by a polymerization reaction of the particles or an aggregation (figure 2). If however a ligand such as

an alkyl amine [30], an alkyl thiol [31], or a carboxylic acid [32] is added the zinc oxide nanoparticles can be stabilized under atmospheric conditions. In this manner it becomes possible to prepare films by coating methods such as spin coating.

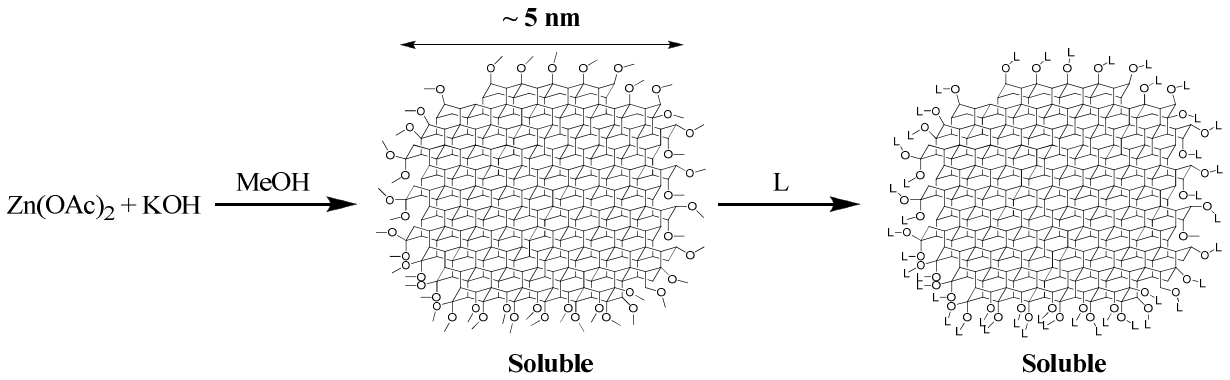

Figure 1. The preparation of zinc oxide nanoparticles in methanol and the exchange of the methoxy groups on the surface with another ligand such as an amine, thiol or a carboxylic acid.

Many ligands were attempted (amines, thiols and carboxylic acids) and the best solution was found to be the alkoxyacetic acids, methoxyacetic acid (MA), methoxyethoxyacetic acid (MEA) and methoxyethoxyethoxyacetic acid (MEEA). MEEA is in many ways well suited but the boiling point is too high to convincingly ensure removal even when heating to 210 ^{o}C and while MA does not have this problem it is quite toxic.

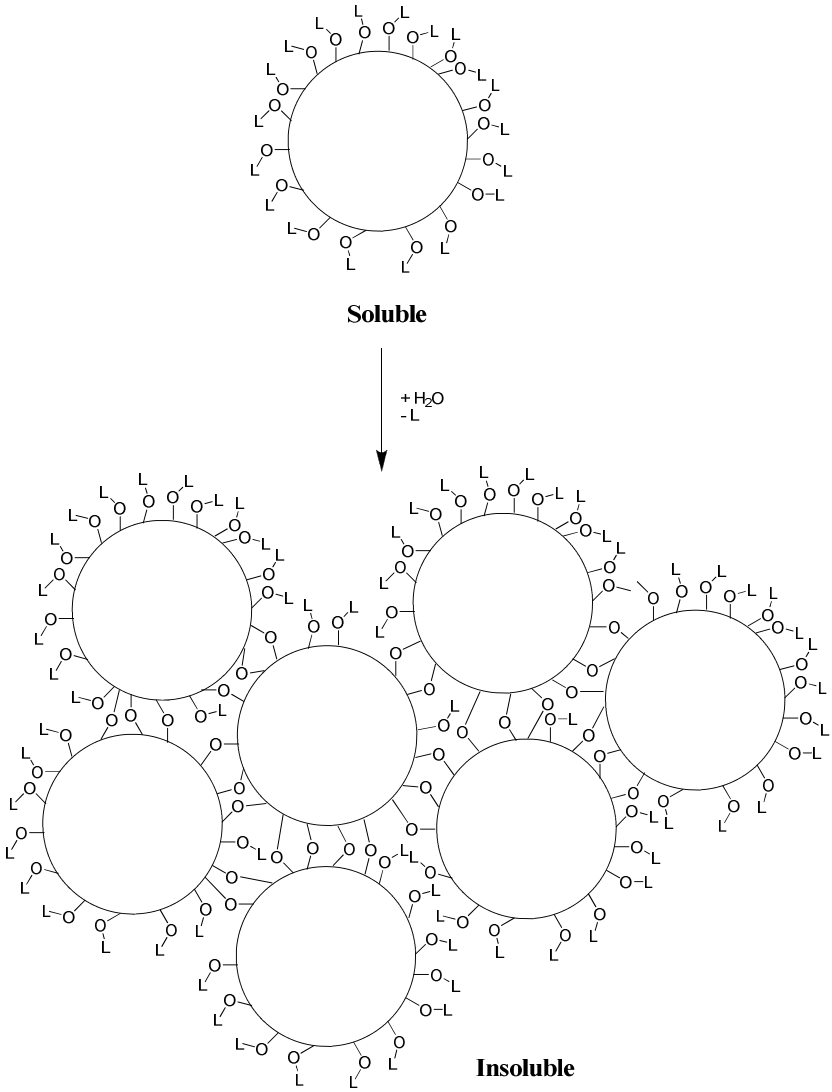

Figure 2. The polymerization reaction or aggregation of the zinc oxide nanoparticles through loss of the ligand on the surface.

The best choice was found to be MEA with a boiling point (at 760 mmHg) of 245 ^{o}C. Addition of MEA to the freshly prepared chlorobenzene/methanol solution of the zinc oxide nanoparticles gave clear solutions that were stable for months under atmospheric conditions. The amount of MEA was not very critical and the highest values employed were 20% (w/w) with respect to the

zinc oxide content in the solution. The high values were however not desirable for two reasons. Firstly, the drying time for the pure zinc oxide films prepared from the solution was longer and required longer curing times at preferably higher temperatures and secondly, when preparing mixtures with P3MHOCT the films prepared by spincoating became opaque due to the poor solubility of P3MHOCT in MEA. During spincoating the lower boiling methanol and chlorobenzene evaporates first leaving the high boiling MEA. When preparing films using 20% (w/w) of MEA with respect to zinc oxide and under the assumption that there is no loss of MEA during evaporation of chlorobenzene and methanol at the concentrations employed means that the final mixture in the film by weight is 12% in MEA, 29% in P3MHOCT and 59% in zinc oxide. Significantly lower concentrations of MEA were required to alleviate this problem while the opacity of the films did not adversely influence device performance. The most serious problem was related to the film adhesion. Zinc oxide films prepared by spincoating the MEA free zinc oxide nanoparticle solution in a glove box required brief heating at 210 ^{o}C to obtain an optically clear insoluble zinc oxide film. When zinc oxide nanoparticle solutions stabilized with 20% (w/w) MEA were spincoated in air clear films were obtained but they remained soluble when heated at 210 ^{o}C for 5 minutes. The sufficient curing times were 60 min at 210 ^{o}C and 5 min at 310 ^{o}C. A good compromise was found to be 4-6% (w/w) MEA with respect to zinc oxide. This allowed for the preparation of optically clear films that required short curing times. When spincoating pure solutions of P3MHOCT in chlorobenzene onto ITO coated glass or PET substrates the polymer film adheres very well and does not scratch off when touched. When cleaved to P3CT, insoluble and even more durable films were obtained. When films of P3MHOCT were prepared in the presence of MEA adhesion was much poorer. At 20% w/w MEA the film could simply be wiped off with paper and significant adhesion for the P3MHOCT

films was first achieved when lowering the MEA concentration to 4-6% w/w which represented a good compromise between stability of the solutions, drying/curing speed, adherence and optical quality of the films.

3.3 Analysis of the materials using transmission electron microscopy

In order to characterize the instability of the zinc oxide nanoparticle solutions, samples with and without MEA stabilization were subjected to TEM analysis. The unstabilized zinc oxide nanoparticle solutions presented large aggregates (several microns) of the smaller nanoparticles as shown in figure 3. It was possible to identify the smaller nanoparticles between the large aggregates and it is a reasonable assumption that the large aggregates are simply very large clusters of the nanoparticles as supported also by X-ray scattering experiments (*vide supra*).

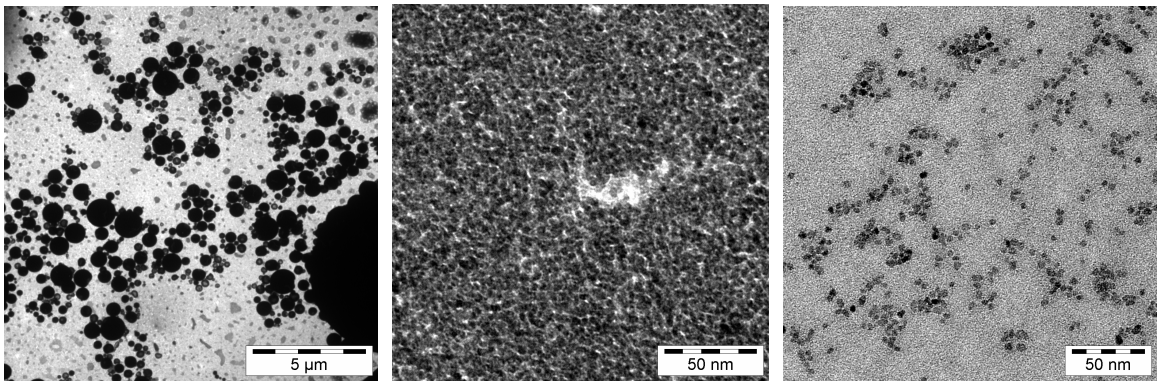

Figure 3. TEM images of the aggregates of zinc oxide nanoparticles that had not been stabilized with MEA (left) and the MEA stabilized zinc oxide nanoparticles at two magnifications (middle and right).

In the case of MEA stabilization the very large aggregates were not observed and well dispersed particles of a very similar size were obtained. Some aggregation at the scale of hundreds of nanometers was however observed as flat structures. The mean particle size was 3.54 ± 0.58 nm as determined by averaging the size of 100 particles observed in the TEM image. In the case of

the dispersions of zinc oxide nanoparticles in the P3CT polymer matrix it was a challenge to obtain good films for TEM. In order to be able to make conclusions on the film morphology from the TEM experiments it is necessary not to affect the film mechanically during preparation of the samples for TEM measurements. It is thus not possible to peel the films mechanically i.e. by a microtome without adversely affecting the film morphology. Instead the films were prepared on glass substrates with a layer of PEDOT:PSS. The film was scored into small squares with a scalpel and submerged into acetone/ethanol whereby the underlayer of PEDOT:PSS dissolves floating the composite film that could then be picked up for TEM analysis. It is a reasonable assumption that the film morphology remains relatively unaffected by this treatment as no mechanical stress is applied to obtain the film.

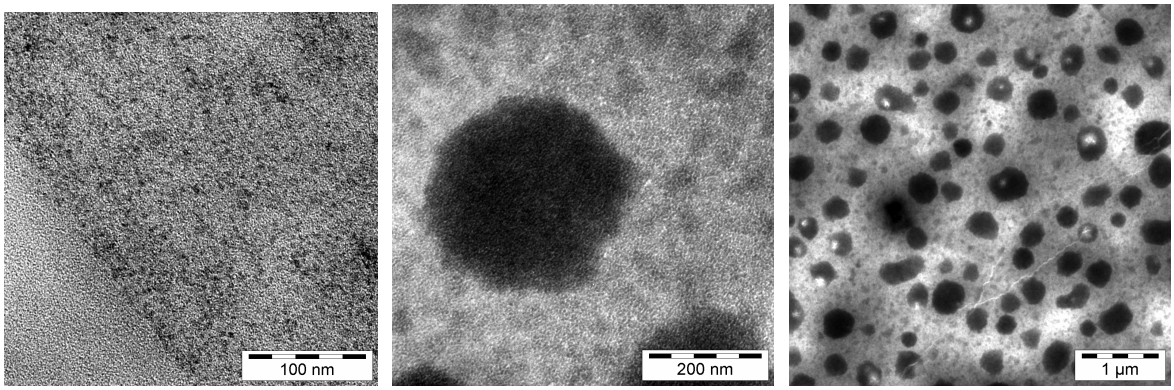

Figure 4. TEM images of the thin films of P3CT and zinc oxide nanoparticles that had been stabilized with MEA. The film thickness was 17 nm. The zinc oxide nanoparticles were well dispersed in the film while larger aggregates were also present. An image where the edge of the film is at the lower right corner of the image shows the well dispersed particles (left). The large aggregates were typically a few hundred nanometers in diameter but (middle and right) but did not protrude beyond the film thickness (17 nm) meaning that they are large disc like aggregates.

However, since solvents were applied to liberate the film from the surface these may affect the film. It is however a reasonable assumption that the solvents employed have had little effect on

film morphology as the thermocleaved films are completely insoluble in the solvent mixture (acetone and ethanol). The films prepared using the concentrations employed for preparing devices, P3CT (25 mg ml^{-1}) and MEA stabilized zinc oxide nanoparticles (50 mg ml^{-1}), were too thick for TEM measurements and a serial dilution of the stock solution was made and the films investigated. Films prepared from 16-fold dilution gave films of a sufficient quality for TEM measurements. The films had a thickness of 17 nm as measured by AFM. Figure 4 shows well dispersed zinc oxide nanoparticles in the P3CT polymer matrix which constitute the device film. It is noteworthy that dense areas of zinc oxide nanoparticles with a diameter of a few hundred nanometers were observed. The thickness of the film was not significantly higher in these areas, i.e. the dense regions are not sphere-like agglomerates of particles, as found for the zinc oxide nanoparticles which had not been stabilized with MEA (figure 3).

3.4 X-ray analysis of the materials using (GI)SAXS, reflectometry and GIWAXS

The SAXS data on solutions confirm that the MEA stabilized zinc oxide particles are in the nanometer size range with a narrow size distribution. The data can be modeled with a unimodal Schulz size distribution of spheres without interaction effects (structure factor), indicating that the particles are well dispersed (figure 5). A weak signal is also observed for the neat polymer solution, more than an order of magnitude weaker than for the neat zinc oxide solution, because of the much smaller electron density contrast between polymer and solvent.

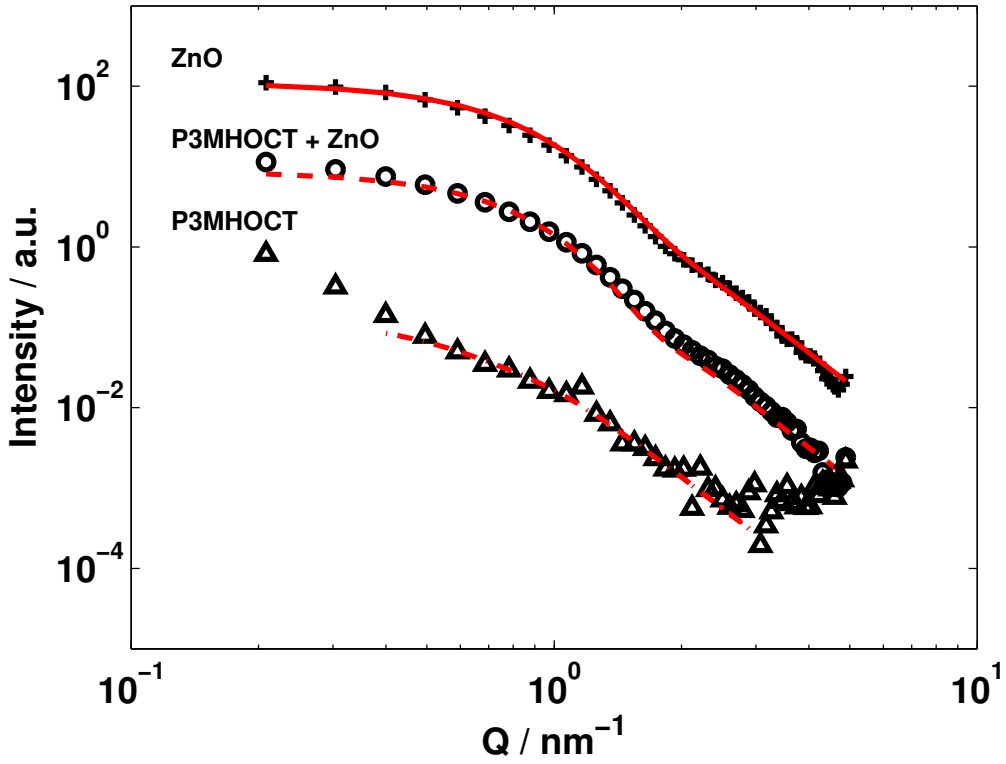

Figure 5. Small angle X-ray scattering cross sections as a function of scattering vector ($Q = 4\pi\sin\theta/\lambda$, θ is half the scattering angle) for solutions in chlorobenzene of zinc oxide nanoparticles, P3MHOCT and a mixture of P3MHOCT and zinc oxide nanoparticles. Lines show the fits, representing polydisperse populations of spheres for the solutions with zinc oxide, and a Guinier/Porod fit for the polymer solution. Data are offset by one or two decades for clarity.

The scattering signal from the solution with both components is completely dominated by the strong scattering from the zinc oxide particles as evident from the close similarity with the scattering cross section of the neat zinc oxide solution. From the fit parameters *r* and *z* of the size distribution,

$$N(r) = \frac{r^{z}}{\Gamma(z+1)}\left(\frac{z+1}{\bar{r}}\right)^{z+1} \exp\left(-\frac{r(z+1)}{\bar{r}}\right)$$

we obtain the root-mean-square deviation, σ_r from the mean size, r, related as $z = (\overline{r}/\sigma_r)^2 - 1$. For the neat zinc oxide solution we find a mean radius of 2.46 nm with σ_r = 0.7 nm. For the zinc oxide/polymer solution, we find r = 2.63 nm and σ_r = 0.7 nm. The distribution width parameter, z, had to be fixed in the refinement by trial and error because it did not refine stably in the least squares procedure. From the combined Guinier/Porod fit of the SAXS data from the polymer solution we find a radius of gyration of 3.1 nm.

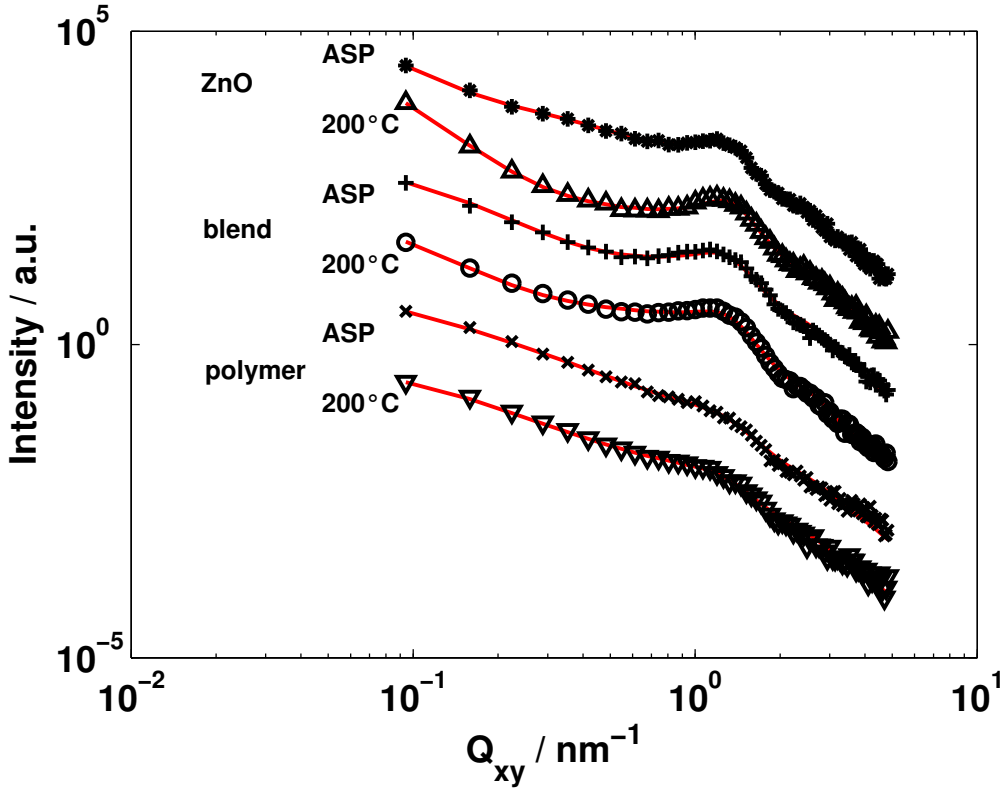

Figure 6. GISAXS data for the films employed in this study ($Q_{xy} = 4\pi\sin\theta/\lambda$, θ is half the scattering angle in the substrate plane, i.e. $\mathbf{Q}_{xy}$ is parallel to the substrate surface). Data for both as prepared (ASP) and heat treated films (200 ^{o}C) are shown for the zinc oxide nanoparticle films, P3MHOCT/P3CT films and the mixture of zinc oxide nanoparticles and P3MHOCT/P3CT. Lines correspond to fits of polydisperse populations of spheres with a hard sphere interaction potential. Data are offset by 1 to 5 decades for clarity.

The GISAXS data reveal clear interaction effects in the thin films, as evidenced by a prominent structure factor peak (figure 6) which indicate particle aggregation. A model of two polydisperse populations of spheres were refined against the data, corresponding to primary particles and their aggregates, with a hard sphere potential describing the interaction. We have summarized the results in table 1. The aggregate sizes are not reported because they are not determined with certainty from these experiments as the defining part of their scattering cross section is outside the experimental resolution (at smaller scattering vectors). We find it particularly noteworthy that the primary particle size of the zinc oxide particles in the thin films is comparable to the sizes found in solutions although slightly smaller for the films as spun. Whether the latter is a real effect or an artifact of the model (including particle interaction for the thin films) is not clear. Another possibility is a larger apparent size in solution because the surface ligands adapt a more extended morphology. In both neat zinc oxide film and in the blend, the mean particle size and polydispersity increase with annealing, whereas the particle interaction radius is unchanged. For the neat zinc oxide film, an increase in scattered intensity at low Q is observed in the annealed film, which we attribute to formation of more large aggregates by sintering. The absence of this effect in the blend thin film could indicate that the polymer inhibits sintering of the zinc oxide particles. A clear structure factor peak is also evident for the neat polymer film, indicating partial crystallization of the polymer corresponding to a d-spacing of 2.2-2.3 nm (table 1). This distance is comparable to lamellar stacking distances (*100*) found for other polythiophene derivatives. The form factor model of polydisperse spheres is likely not meaningful for the polymer morphology, but was applied to facilitate the structure factor fitting. In case of the neat polymer film, the

values for radius of scatterer and polydispersity should therefore not be ascribed particular significance. A full treatment of polymer morphology is outside the scope of this study.

Table 1. Structural parameters for the spin coated thin films, determined from GISAXS, X-ray reflectometry and GIWAXS. All figures are given in nm. Figures in parentheses are estimated uncertainties on the last significant digit.

	ZnO, as spun	**ZnO, 200°**	**P3MHOCT, as spun**	**P3CT, 200°**	**P3MHOCT/ZnO, as spun**	**P3CT/ZnO, 200°**
Mean radius of scatterer	1.79	2.37	1.79 (polymer)	1.24 (polymer)	1.66	2.27
σ_r	1.02	1.92	6.0[1]	6.0[1]	0.86	1.16
Interaction radius	2.26	2.37	2.24 (polymer)	2.29 (polymer)	2.30	2.31
Film thickness	n.d.[2]	28(2)	40(1)	37(1)	88(5)	74(5)
Majority ZnO polytype	zincblende	zincblende	-	-	wurtzite	zincblende

[1]Fixed by trial and error, because it did not refine stably in the least squares procedure.

[2]This film was apparently too inhomogeneous and rough to give well defined Kiessig fringes.

Except for the neat zinc oxide film as spun, the reflectivity measurements yielded sufficiently well defined Kiessig fringes to allow determination of film thickness (figure 7). The derived

thickness values are reported in table 1 and show that spin coating of the blend solution apparently results in films about three times thicker than the neat zinc oxide films and about double the thickness of neat polymer films. The neat polymer film shrinks by about 10% during annealing and the blend film by about 15%, somewhat less than recently found for a comparable system [33].

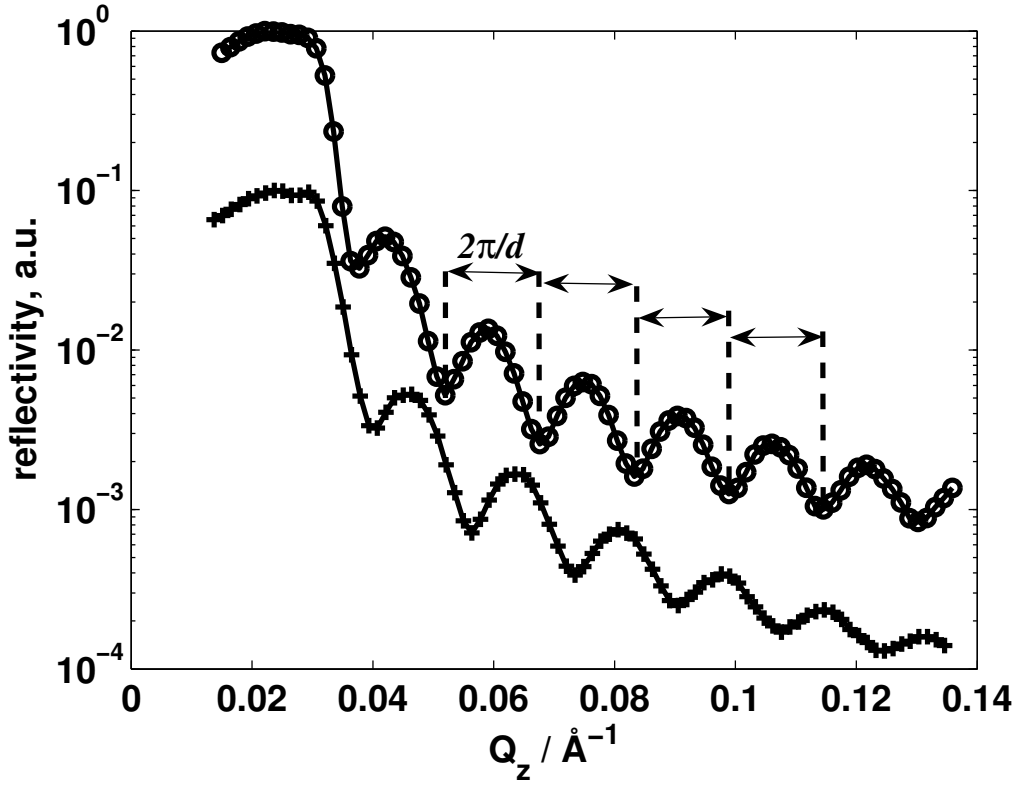

Figure 7. Reflectivity profiles for films of P3MHOCT (open cicrles) and P3CT (crosses), offset by a decade for clarity. $Q_z = 4\pi\sin\theta/\lambda$, θ is half the scattering angle in the specular scattering plane (**Q** parallel to surface normal).

The GIWAXS measurements shows very broad crystalline peaks from the zinc oxide nanoparticles and a broad peak at Q~1.36 Å^{-1} corresponding to a d-spacing of ~4.62 Å which we ascribe to the polymer "π-stack".

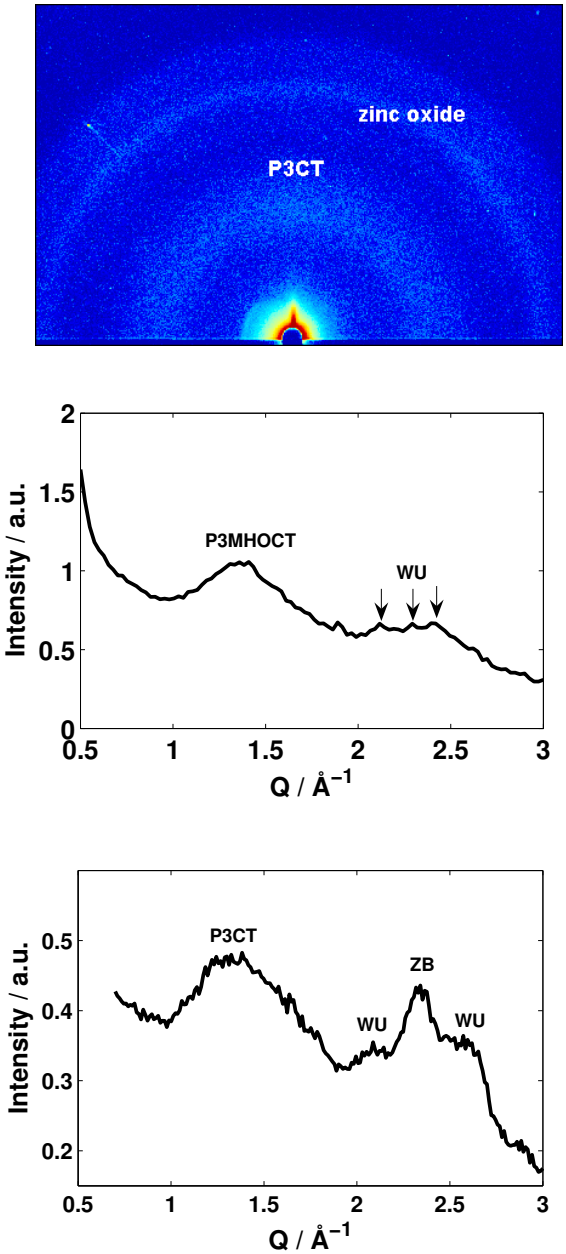

Figure 8. GIWAXS data of the zinc oxide/polymer composite films. The data as recorded for the heat treated film show a uniform distribution of zinc oxide reflection intensity and thus no preferred orientation of zinc oxide particles in the film, whereas the slightly anisotropic distribution of scattered intensity from the polymer indicate some texturing. (top, log scale). The as prepared film of P3MHOCT and zinc oxide nanoparticles show mainly the wurtzite structure (middle) and after the heat treatment a mixture of zincblende and wurtzite is observed (bottom).

The 2D data reveal an atypical texture for spin coated films of polythiophene with the π-stack diffracting along the direction of the surface normal, corresponding to the polymer chains lying on the substrate with the aromatic planes parallel to the surface as is more typical for drop cast films [34]. The isotropic distribution of intensity along the zinc oxide diffraction rings indicates that the nanoparticles do not adopt a preferred orientation (figure 8, top). Although difficult to elucidate from the broad and weak zinc oxide reflections, it appears that the nanoparticles in the blend film as spun, predominantly adopt the wurtzite structure, which is the normal zinc oxide structure for bulk material (figure 8, middle). Remarkably, however, zincblende is the dominant polytype in the annealed film, and in the neat zinc oxide film, as spun and annealed (figure 8, bottom and table 1). We are only aware of two other studies where zinc oxide has been found to adopt this polytype [35,36]. A modification of the nanoparticle surface energy by the ligands may be responsible for the stabilization of this uncommon polytype. The crystallinity is significantly improved by the annealing process cf. the stronger, better resolved reflections from the annealed film (figure 8, bottom) as compared to the film as spun (figure 8, middle).

3.5 Preparation of devices

Polymer, hybrid and small molecule organic solar cells traditionally involve the use of one or more vacuum coating steps. Most notably the vacuum coating step is associated with completion of the device by evaporation of a back metal electrode. In many cases that back electrode is a reactive metal such as aluminium or calcium and the protection of the device from the atmosphere during preparation of the active layers of the device and after completion of the device by evaporation of the back electrode must be considered common. In the case of the devices presented here the entire device preparation is performed in the ambient atmosphere. We

consider it a strength that this procedure enable the preparation of devices without the need for a glove box environment or vacuum equipment. The device geometry is shown schematically in figure 9 along with a photograph of the finished devices on glass substrates and on PET. The devices comprise a first layer of zinc oxide obtained by spincoating a solution of the soluble zinc oxide nanoparticles directly onto the conducting ITO substrate followed by annealing of the layer to an insoluble form by short heating at high temperature or by longer heating times at lower temperatures.

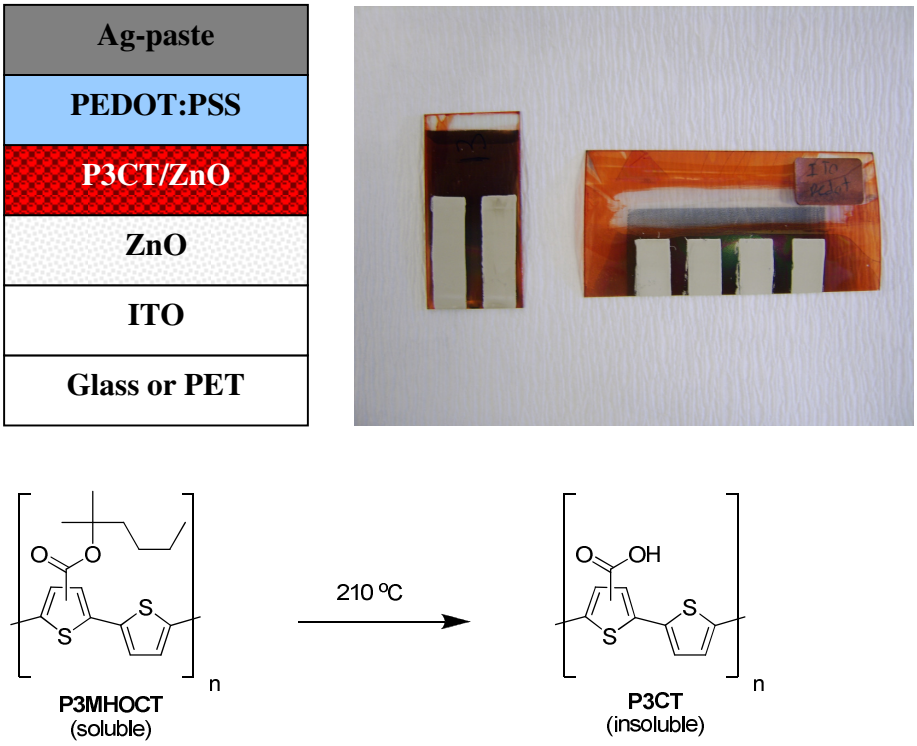

Figure 9. A schematic illustration of the device geometry (left) and photographs of the devices on rigid glass (middle) and flexible PET (right) substrates. The thermal conversion of P3MHOCT to P3CT is shown in the lower part of the figure.

The insolubility arises as the nanoparticles aggregate by loss of the solubilising ligand shown in figure 2. In an earlier report [20] this type of device was prepared under glovebox conditions using methanol as the ligand. In this case the aggregation is immediate upon heating to 200 ^{o}C where the loss of methanol is fast. In this case the ligand MEA is lost more slowly and the aggregation is much slower. The insoluble film consist of aggregated nanoparticles as evidenced by SAXS on the films and it is thus not a dense zinc oxide layer. The active layer is spincoated on top of the zinc oxide electrode and comprise initially a composite of the soluble polymer P3MHOCT and the soluble MEA stabilized zinc oxide nanoparticles. The film is heated to 210 ^{o}C to convert soluble P3MHOCT to insoluble P3CT and possibly also initiate some sintering of the zinc oxide nanoparticles. The device is then completed by spincoating or screen printing a layer of PEDOT:PSS followed by application of a silver paste back electrode. The preparation of the devices on glass where heating is quite fast can be completed in less than 15 minutes. In the case of PET substrates much longer times are required since the annealing time of the first zinc oxide layer and the thermocleavage of P3MHOCT to P3CT is much slower at the temperatures that PET can withstand. PET is typically not mechanically stable at temperatures above 150 ^{o}C. In this study the upper temperature for PET substrates was kept at 140 ^{o}C. One of the advantages of the silver paste back electrodes is that they are mechanically quite durable and unlike evaporated electrodes there are no special requirements for handling them. They are scratch proof and are only damaged if one makes an effort.

3.6 Device performance and stability

One of the distinguishing features of all organic solar cells is that they often degrade rapidly when operated in contrast to most traditional semiconductor based solar cells. The degradation and failure mechanisms are many and a complex interplay exists between them as reviewed

recently [37]. Quite often scientific reports on the marvelous nature of polymer and organic solar cells do not mention stability and in many cases this would also have made the reports less marvelous. Some work dedicated to understanding of the degradation have however led to crude knowledge on why devices break down and this has enabled the preparation of devices with stable operation for many thousands of hours under continuous illumination and elevated temperature [38-40]. It should be emphasized that so far all stable operation has been under the exclusion of oxygen and water from the atmosphere except for the type of device reported here.

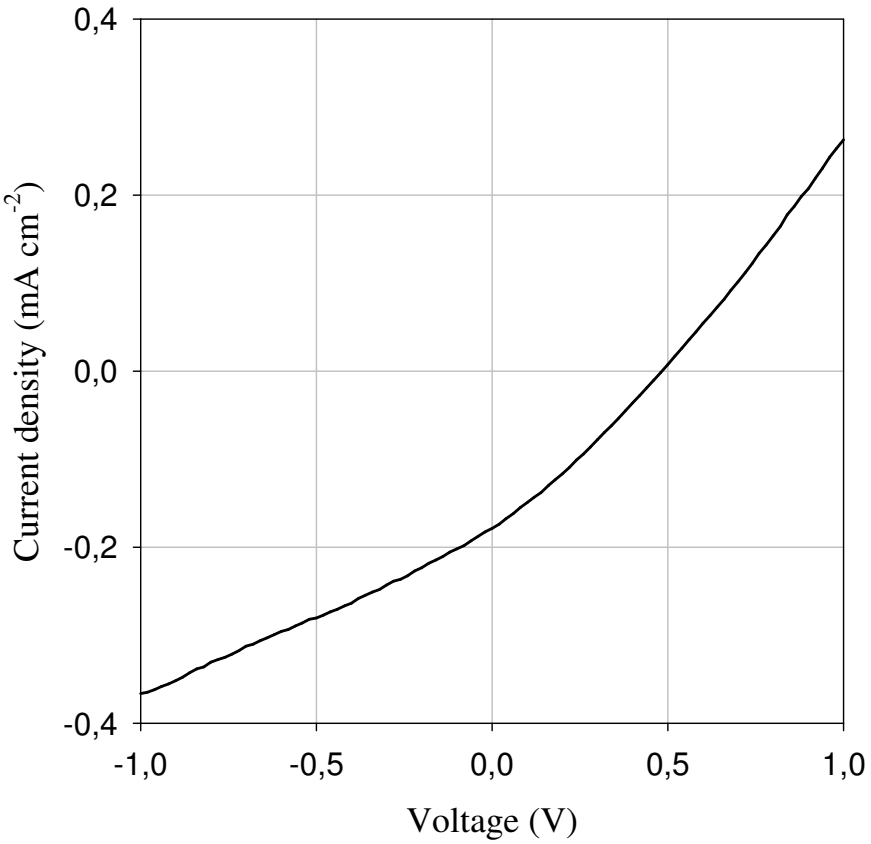

Figure 10. IV chracteristics of an as prepared device on a glass substrate with and active area of 1 cm^2. Test conditions were 1000 W m^{-2}, AM1.5G, 72 ± 2 °C, 35 ± 5 % relative humidity, ambient atmosphere.

Even though the performance of this technology is inferior to the state of the art in terms of efficiency it is considered a breakthrough that a polymer device with moderately stable operation in air can be prepared. In this report both the preparation and operation of the device is carried out in the ambient atmosphere without any efforts in the direction of protecting the device from the atmospheric components (i.e. no encapsulation in any form). In terms of efficiency the devices reported earlier were partly prepared under inert conditions but the operation was in the ambient atmosphere. In the latter case the device improved significantly upon standing in the dark or under illumination after being introduced to the atmosphere. It was of some interest to see if this was also the case here as these devices are prepared in the ambient atmosphere it was anticipated that there should be no maturing effect as such.

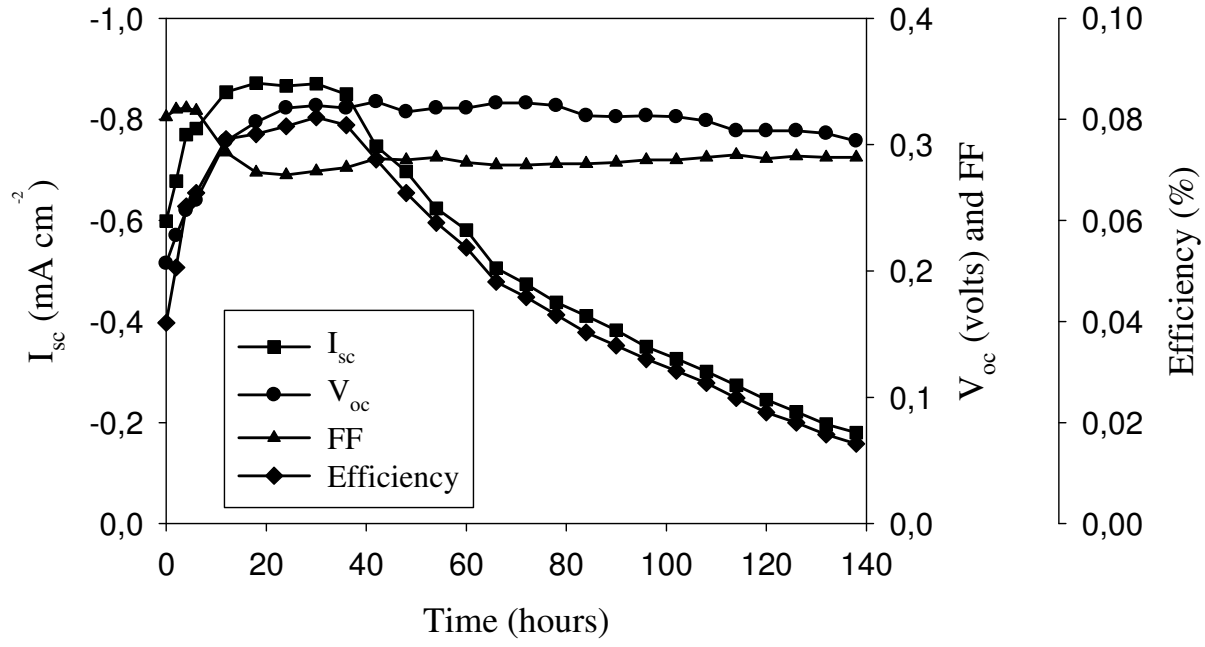

Figure 11. Evolution of I_{sc}, V_{oc}, FF and the efficiency as a function of time during continuous light soaking (1000 W m^{-2}, AM1.5G, 72 ± 2 ^{o}C, 35 ± 5 % relative humidity, ambient atmosphere, no encapsulation).

This was partly confirmed as the devices gave a reasonable current and a high voltage to begin with (figure 10). The devices were however also subject to annealing during the first 20-50 hours of operation where the current increased significantly by as much as a factor of 2. In terms of efficiency this type of device performs quite poorly under illumination at 1 sun. There is however a strong non-linear behavior of the power conversion efficiency with the incident light intensity and under low light conditions the efficiency is as high as 0.5%. While still a low value it should be noted that it is stable in operation in ambient air which is unprecedented. It is very likely that the morphology and the carrier transport can be improved in this type of devices thus improving the performance. In terms of the stability the results are comparable to the earlier report even though it must be anticipated that the MEA stabilized zinc oxide nanoparticles could behave quite differently from the unstabilized particles. The results of continuous light soaking under accelerated conditions are shown in figure 11. The conditions of the lifetime test is quite harsh and as shown earlier [20] lower temperatures significantly improve the lifetime. The device type prepared here is quite stable on standing and while the operational lifetime must be considered relatively short the performance and lifetime under lower light pressures and temperatures make this excellently suited for demonstration purposes and perhaps small applications.

4. Conclusion

A nanostructured polymer solar cell comprising a thermocleavable polymer material and zinc oxide nanoparticles was presented. The zinc oxide nanoparticles were stabilized such that all manipulations during device preparation could be carried out in air without the need for vacuum steps. Only simple equipment is required to prepare this type of device that may well serve as a teaching example. The morphology of the device films and materials were characterized by TEM

and X-ray scattering techniques showing that the particles were well dispersed and quite homogenous with respect to particle size. Large aggregates of nanoparticles were present in the films while the local structure presented a good dispersion of the smaller particles in the polymer matrix. The devices could be operated in the ambient atmosphere and the performance of the devices during continuous illumination (1000 W m^{-2}, AM1.5G, 35 ± 5% relative humidity, 72 ± 2 ^{o}C) decreased to 80 % of the initial performance in approximately 100 hours.

Acknowledgements

This work was further supported by the Danish Strategic Research Council (DSF 2104-05-0052 and DSF-2104-07-0022).

References

† A patent application covering this invention has been filed

[1] Grätzel M 2005 Dye-sensitized solid state heterojunctions solar cells *MRS Bulletin* **30** 23-27

[2] O'Regan B and Grätzel M 1991 A low cost, high efficiency solar-cell based on dye-sensitized colloidal TiO_2 films *Nature* **353** 737-40

[3] Forrest SR 2005 The limits to organic photovoltaic cell efficiency *MRS Bulletin* **30** 28-32

[4] Rand B P, Genoe J, Heremans P and Poortmans J 2007 Solar cells utilizing small molecular weight organic semiconductors *Prog. Photovolt: Res. Appl.* **15** 659–76

[5] Janssen R A J, Hummelen J C and Sariciftci N S 2005 Polymer-fullerene bulk heterojunctions solar cells *MRS Bulletin* **30** 33-6.

[6] Günes S, Neugebauer H and Sariciftci N S 2007 Conjugated polymer-based organic solar cells *Chem. Rev.* **107** 1324-38.

[7] Milliron D, Gur I and Alivisatos A P 2005 Hybrid organic-nanocrystal solar cells *MRS Bulletin* **30** 41-4.

[8] Coakley K M, Liu Y, Goh C and McGehee M D 2005 Ordered organic-inorganic bulk heterojunctions photovoltaic cells *MRS Bulletin* **30** 37-40

[9] Grätzel M 2005 Mesoscopic solar cells for electricity and hydrogen production from sunlight *Chem. Lett.* **34** 8–13

[10] Xue J, Uchida S, Rand B P and Forrest SR 2004 4.2% efficient organic photovoltaic cells with low series resistances *Appl. Phys. Lett.* **84** 3013-5

[11] Li G, Shrotriya V, Huang J, Yao Y, Moriarty T, Emery K and Yang Y 2005 High-efficiency solution processable polymer photovoltaic cells by self-organization of polymer blends *Nature Materials* **4** 864-8

[12] Ma W, Yang C, Gong X, Lee K and Heeger A J 2005 Thermally Stable, Efficient Polymer Solar Cells with Nanoscale Control of the Interpenetrating Network Morphology *Adv. Funct. Mater.* **15** 1617-22

[13] Cherepy N J, Smestad G P, Grätzel M and Zhang J Z 1997 Ultrafast electron injection: implications for a photoelectrochemical cell utilizing an anthocyanin dye-sensitized TiO_2 nanocrystalline electrode *J. Phys. Chem.* **101** 9342-51

[14] Smestad G P and Grätzel M 1998 Demonstrating Electron Transfer and Nanotechnology: A natural dye-sensitized nanocrystalline energy converter *J. Chem. Education* **75** 752-6

[15] Smestad G P 1998 Education and solar conversion: demonstrating electron transfer *Sol. Energ. Mater. Sol. Cells* **55** 157-78

[16] H. Womelsdorf, W. Hoheisel, G. Passing, Nanopartikuläres, redispergierbares fällungsoxid, German Patent (filing date 23.02.1999), DE 19907704 A1.

[17] H. Womelsdorf, W. Hoheisel, G. Passing, Process for producing nanoparticulate, redispersible zinc oxide gels, European patent (filing date 11.02.2000) EP 1157064 B1.

[18] H. Womelsdorf, W. Hoheisel, G. Passing, Nanoparticulate, redispersible zinc oxide gels, Unites States patent (patent date 23.03.2004) US 6,710,091 B1

[19] Beek W J E, Wienk M M, Kemerink M, Yang X and Janssen R A J 2005 Hybrid zinc oxide conjugated polymer bulk heterojunctions solar cells *J. Phys. Chem. B* **109** 9505-16

[20] Krebs F C 2008 Air stable polymer photovoltaics based on a process free from vacuum steps and fullerenes *Sol. Energ. Mater. Sol. Cells* doi:10.1016/j.solmat.2008.01.013

[21] Liu J S, Kadnikova E N, Liu Y X, McGehee M D and Fréchet J M J 2004 Polythiophene containing thermally removable solubilizing groups enhances the interface and the performance of polymer-titania hybrid solar cells *J. Am. Chem. Soc.* **126** 9486-7

[22] Levine J, Cohen J B, Chung Y W and Georgopoulos P 1989 Grazing-incidence small-angle X-ray scattering: new tool for studying thin film growth *J. Appl. Cryst.* **22** 528-32

[23] Schulz G V 1939 Über die Kinetik der Kettenpolymerisationen. V *Z. Phys. Chem. B.* **43** 25-46

[24] Zimm B H 1948 Apparatus and Methods for Measurement and Interpetration of the Angular Variation of Light Scattering; Preliminary Results on Polystyrene Solutions *J. Chem. Phys.* **16** 1099-116

[25] Beaucage G and Schaefer D W 1994 Structural Studies of Complex-Systems Using Small-Angle Scattering - A Unified Guinier Power-Law Approach *J. Non-Cryst. Solids* **172** 797-805

[26] Baxter R J 1968 Percus-Yevick Equation for Hard Spheres with Surface Adhesion *J. Chem. Phys.* **49** 2770-4

[27] Konarev P V, Volkov V V, Sokolova A V, Koch M H J and Svergun D I 2003 PRIMUS: a Windows PC-based system for small-angle scattering data analysis *J. Appl. Cryst.* **36** 1277-82

[28] Kiessig H 1931 Interferenz von Röntgenstrahlen an dünnen Schichten *Ann. Phys.* **5** 769-88

[29] Apitz D, Bertram R P, Benter N, Hieringer W, Andreasen J W, Nielsen M M, Johansen P M and Buse K 2005 Investigation of chromophore-chromophore interaction by electro-optic measurements, linear dichroism, x-ray scattering, and density-functional calculations *Phys. Rev. E.* **72** 036610

[30] Kahn M L, Monge M, Colliére V, Senocq F, Maisonnat A and Chaudret B 2005 Size- and shape-control of crystalline zinc oxide nanoparticles: A new organometallic synthetic method *Adv. Funct. Mater.* **15** 458-68

[31] Pesika N S, Hu Z, Stebe K J and Searson P C 2002 Quenching of growth of ZnO nanoparticles by adsorption of octanethiol *J. Phys. Chem. B* **106** 6985-90

[32] Sakohara S, Ishida M and Anderson M A 1998 Visible luminescence and surface properties of nanosized ZnO colloids prepared by hydrolyzing zinc acetate *J. Phys. Chem. B* **102** 10169-75

[33] Andreasen J W, Jørgensen M and Krebs F C 2007 A route to stable nanostructures in conjugated polymers *Macromolecules* **40** 7758-62

[34] Sirringhaus H, Brown P J, Friend R H, Nielsen M M, Bechgaard K, Langeveld-Voss B M W, Spiering A J H, Janssen R A J, Meijer E W, Herwig P and de Leeuw D M 1999 Two-

dimensional charge transport in self-organized, high-mobility conjugated polymers *Nature* **401** 685-688

[35] Bragg W L and Darbyshire J A 1932 The structure of thin films of certain metallic oxides *Transactions of the Faraday Society* **28** 522-28

[36] Snedeker L P, Risbud A S, Ombretta M, Zhang J P and Seshadri R 2005 Organic phase conversion of bulk (wurtzite) ZnO to nanophase (wurtzite and zinc blende) ZnO *Solid State Sciences* **7** 1500-5

[37] Jørgensen M, Norrman and Krebs F C 2008 Stability/degradation of polymer solar cells doi:10.1016/j.solmat.2008.01.005

[38] Yang X, Loos J, Veenstra S C, Verhees V J H, Wienk M M, Kroon J M, Michels M A J and Janssen R A J 2005 Nanoscale morphology of high-performance polymer solar cells *Nanolett.* **4** 579-83

[39] Krebs F C and Spanggaard H 2005 Significant improvement of polymer solar cell stability *Chem. Mater.* **17** 5235-7

[40] Krebs F C and Norrman K 2007 Analysis of the failure mechanism for a stable organic photovoltaic during 10 000 h of testing *Prog. Photovolt.: Res. Appl.* **15** 697-712